

# Plastic Mechanism and Elastic Analyses in the Strength Estimation of an Axially Compressed-Thin-Walled Channel Steel Section Beam

Harkali Setiyono

*Technology Center for Structural Strength*

*Agency for the Assessment and Application of Technology ( B2TKS – BPPT )*

*Kompleks PUSPIPTEK Serpong-Tangerang 15314, Indonesia*

*E-mail: harkali@luk.or.id*

**ABSTRACT:** This paper presents the study of an analytical model to estimate the strength of a thin-walled channel steel section beam subjected to axial-compressive loads. The model is based on two different methods of analysis, which are performed by analysing a plastic failure mechanism and elastic behaviour of the beam. These analytical methods can be used to establish plastic-unloading and elastic-inclining-theoretical load-deflection behaviour of the beam. Meanwhile, the axial-compressive strength of the beam is estimated by directly measuring the value of load at an intersection point between two different curves of the theoretical load-deflection behaviour. The accuracy of using this analytical model is also verified by comparing its estimated data of the strength to the one obtained from a number of tests on 38 specimens of thin-walled channel steel section under the test loads of axial compression. It is clearly shown that deviation of the analytical data from the experimental one is still scattered within acceptable limits of  $\pm 20\%$ . A statistical analysis of the scattered data indicates that its mean value is 1.03 with standard deviation of 0.058. This certainly means that the estimated strength, on average, displaces from the actual one by 3% and mostly tends to be conservative.

**KEYWORDS:** Channel section, local buckling, plastic mechanisms, effective width, moment capacity and axial-compressive strength

## 1. INTRODUCTION

An analytical model of combined plastic mechanism and elastic approaches has been developed to estimate the strength of a thin-walled channel steel section beam subjected to axial-compressive loads. It has been encountered from literature reviews that a failure process of a thin-walled steel section under applied loads is generally initiated by the formation of local buckling on its compressed elements, which subsequently can develop to be local plastic failure mechanisms at collapse. In the plastic mechanism analysis, a plastic failure mechanism of the beam affected by the axial-compressive loads is analysed according to a concept of energy equilibrium between work done by virtual displacement of applied loads and energy dissipating in plastic hinges of the mechanism during deformation. The dissipated energy is determined on the basis of moment resisting capacity of plastic hinges and their appropriate rotations. This energy equilibrium is

then analysed in more detail in order to get an expression of load carrying capacity of the beam in term of its axial deflection. Using the expression of load carrying capacity, an unloading curve of theoretical load-deflection behaviour can be produced and it is called in this paper as a plastic mechanism curve. In some literatures <sup>(Murray 1981-1986)</sup>, this curve will approximate post-collapse behaviour of the investigated beam. The plastic failure mechanisms of the beam can be recognized from very careful observation on a number of thin-walled channel steel sections tested to failure in our laboratory. Figure 8 shows a type of failure mechanism of the sections and it can be seen in the Figure that the plastic failure mechanism is composed of six plastic hinges, i.e. two plastic hinges in the form of flip-disc mechanism in the web element and another four ones in both sides of the flange element. In case of elastic analysis, the effect of local buckling is taken into account in the analysis. This consideration needs to be taken because the existence of local buckling on the

affected elements of the beam causes them to be less effective in carrying applied loads. Figure 1 illustrates the effect of local buckling on the elastic stress distribution in a compressed web element of a thin-walled channel section subjected to bending moments (Rhodes 1991). On the basis of the illustration, an effective width concept should be used to determine element widths of the investigated beam, which are still effective in carrying the applied-compressive loads.

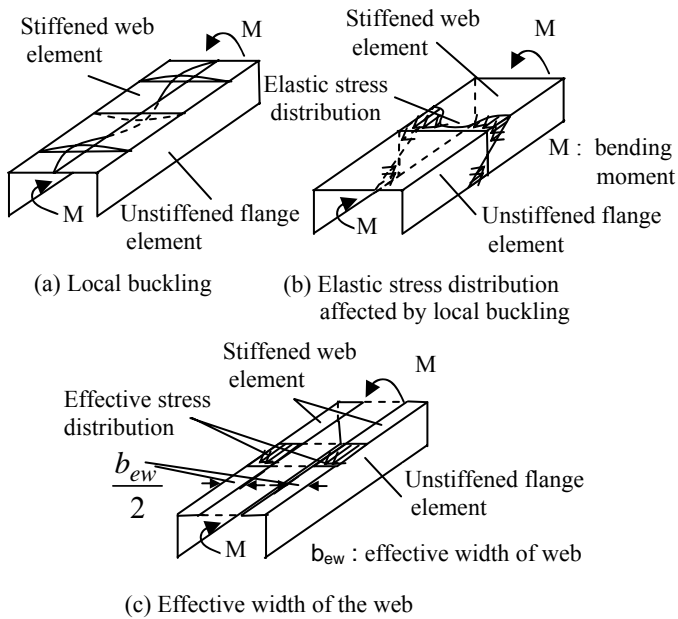


Figure 1. Effect of local buckling (Rhodes 1991).

Utilization of the effective element widths in the elastic analysis results in another formulation of load carrying capacity in term of axial deflection. Using this formulation, a theoretically inclining load-deflection behaviour of the beam, which is called an elastic curve in this paper, can be established and this will be able to predict actual elastic load-deflection one. The axial-compressive strength of the investigated beam is predicted by adopting a method of cut-off strength (Bakker 1990, Setiyono 1994-2003), as shown in Figure 2, where the value of load at the intersection of the plastic mechanism and elastic curves is assumed to be theoretical-axial-compressive strength of the beam. Beyond the analytical approaches, the axial-compressive strength of the beam is also experimentally assessed and results obtained are used to verify the analytical predictions. In this paper, scattered deviation between analytical and experimental data is limited within tolerances of  $\pm 20\%$  and the degree of accuracy is assessed by using a statistical analysis of the scattered data populations. The accuracy of theoretical load-deflection behaviour in predicting the actual one is also demonstrated at the end of this paper.

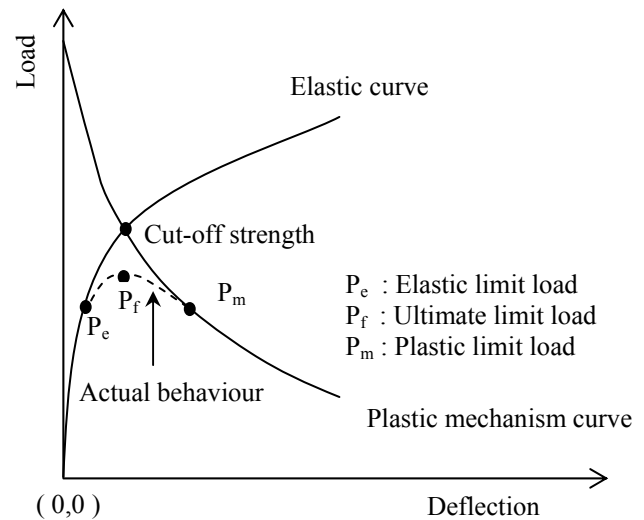


Figure 2. Method of cut-off strength (Bakker 1990, Setiyono 1994-2003).

## 2. ANALYTICAL APPROACH

The analytical approach was carried out in two stages where the first stage is a plastic analysis of a plastic mechanism model as shown in Figure 3 and the second one is an elastic analysis of the beam. Both analyses are mainly aimed at developing two different formulations of plastic and elastic load carrying capacity with respect to axial deflection or axial shortening. Using these formulations, approximated load-deflection behaviour of the beam, especially in elastic and post-collapse regions, can be established and its axial-compressive strength can also be directly estimated according to the method of cut-off strength in Figure 2. In order to be able to use the method of cut-off strength, a computer program was written to iterate the formulations in generating two different curves of plastic mechanism and elastic behaviour. The iteration was performed by firstly setting the value of axial shortening to zero and incrementally increasing it until both values of plastic and elastic load carrying capacity to converge in a point. The value of load carrying capacity at this point is then theoretically assumed to be the axial-compressive strength of the beam.

### 2.1 Plastic Mechanism Analysis

The plastic mechanism model indicated in Figure 3 is an idealization of the plastic failure mechanism of the beam in Figure 8. In the Figure 3, the axial-compressive loads ( $F_{ax}$ ) are assumed to be applied at point c so that the beam is fully subjected to purely axial-compressive loads without additional bending. The plastic analysis of the model is based on a

concept of energy equilibrium, which is formulated as follows:

$$E_{ext} = \sum_{i=1}^{i=n} [(M_p^1)_i \cdot \theta_i] \quad (1)$$

Where :

- $E_{ext}$  : external energy and it is equal to work done by the virtual displacement of applied loads  $F_{ax}$
- $M_p^1$  : reduced-plastic moment capacity of each plastic hinge
- $\theta$  : rotation angle of each plastic hinge during deformation

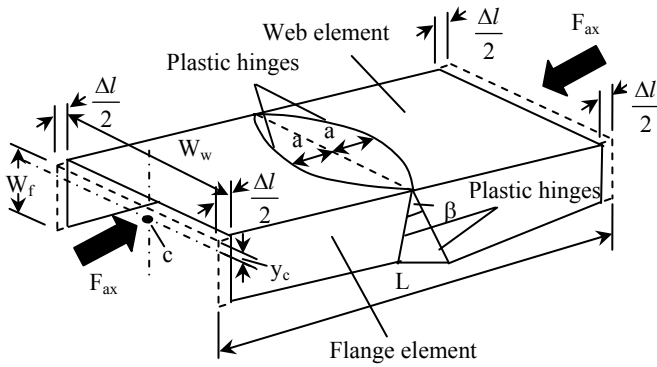


**Figure 3. Idealized-plastic failure mechanisms of the investigated beam.**

The right hand side term of equation (1) expresses the sum of energy dissipation in plastic hinges and on the basis of N.W. Murray's formulation <sup>(Murray 1981-1986)</sup>, the reduced-plastic moment capacity of the plastic hinge that is perpendicular to the direction of applied load  $F_{ax}$  is calculated from:

$$M_p^1 = \frac{\sigma_y b t^2}{4} \left[ 1 - \left( \frac{F_{ax}}{\sigma_y b t} \right)^2 \right] \quad (2)$$

$\sigma_y$  is material yield strength while  $b$  and  $t$  are the length and thickness of the plastic hinge respectively. When the plastic hinge is oriented at an angle of  $\alpha$  to the direction of the applied load  $F_{ax}$ , the reduced-plastic moment capacity ( $M_p^{111}$ ) becomes as follows:

$$M_p^{111} = M_p^1 \sec \alpha = \frac{\sigma_y b t^2}{4} \left[ 1 - \left( \frac{F_{ax}}{\sigma_y b t} \right)^2 \right] \sec \alpha \quad (3)$$

The formulae of (2) and (3) are basically used in determining the reduced-plastic moment capacity of all plastic hinges throughout the plastic analysis of the mechanism model in Figure 3. If under the applied-axial-compressive loads  $F_{ax}$  the beam shortens by  $\Delta l$ , the work done by the load  $F_{ax}$  is therefore equal to the product of  $F_{ax}$  and  $\Delta l$ . Meanwhile, the energy dissipating in plastic hinges is the sum of energy absorbed by the plastic hinges in the web and flange mechanisms so that the equation (1) may be rewritten as follows:

$$F_{ax} \Delta l = (E_{dis})_w + (E_{dis})_f \quad (4)$$

$(E_{dis})_w$  and  $(E_{dis})_f$  are the energy absorbed by the plastic hinges in the web and flange mechanisms where they are calculated according to the sum of the product of the reduced plastic moment capacity and the rotation angle at each plastic hinge of both mechanisms. The energy dissipated in the web and flange mechanisms can be obtained from the following expressions.

$$(E_{dis})_w = \tan^{-1} \left( \frac{2a - \Delta l}{\sqrt{\Delta l(4a - \Delta l)}} \right) [F_1 - F_2] \quad (5)$$

$$F_1 = \frac{0.045 \sigma_y t^2 W_w^2}{a} \left\{ \ln \tan \left( \frac{\pi}{4} + \frac{\phi_1}{2} \right) - \ln \tan \left( \frac{\pi}{4} + \frac{\phi_2}{2} \right) \right\}$$

$$F_2 = \left\{ \frac{a(W_f - 2y_c)^2 F_{ax}^2}{0.72 \sigma_y W_f^2 W_w^2 \left\{ \ln \tan \left( \frac{\pi}{4} + \frac{\phi_1}{2} \right) - \ln \tan \left( \frac{\pi}{4} + \frac{\phi_2}{2} \right) \right\}} \right\}$$

$$(E_{dis})_f = \frac{\{(0.866 \sigma_y t W_f^2)^2 - (y_c F_{ax})^2\} (\theta_1 + \theta_2)}{1.73 \sigma_y W_f^3} \quad (6)$$

In the formulae of (5) and (6), parameters of  $\phi_1$ ,  $\phi_2$ ,  $\theta_1$  and  $\theta_2$  are the inverse tangent of factors as formulated in equations (7) and (8). Meanwhile,  $y_c$  is the position of center  $c$  from the web element and it is expressed as in equation (9).

$$\phi_1 = \tan^{-1}(F_3) \quad ; \quad \phi_2 = \tan^{-1}(F_4) \quad (7)$$

$$F_3 = \frac{5.66 a}{\sqrt{4W_w^2 - 32a^2}} \quad ; \quad F_4 = \frac{-5.66 a}{\sqrt{4W_w^2 - 32a^2}}$$

$$\theta_1 = \tan^{-1} \left( \frac{\sqrt{1-x_1^2}}{x_1} \right) \quad ; \quad \theta_2 = \tan^{-1} \left( \frac{\sqrt{1-x_2^2}}{x_2} \right) \quad (8)$$

$$y_c = \frac{W_f^2}{(2W_f + W_w)} \quad (9)$$

Where:

$$x_1 = \frac{(A^1 B^1)^2 + (A^1 C^1)^2 - (B B^1)^2 - (B C^1)^2}{2(A^1 B^1)(A^1 C^1)} + \frac{2(B B^1)(B C^1) \cos \beta_2}{2(A^1 B^1)(A^1 C^1)}$$

$$A^1 B^1 = \frac{0.43 W_f A D \sqrt{3W_f^2 - A D^2}}{1.5W_f^2 - A D^2}$$

$$A D = W_f \sqrt{\frac{0.75L - 1.16\sqrt{\Delta l(4a - \Delta l)}}{L}}$$

$$A^1C^1 = 0.75W_f$$

$$BB^1 = \frac{0.65W_f L}{0.75L + 1.16\sqrt{\Delta l(4a - \Delta l)}} ; BC^1 = 0.866W_f$$

$$\cos \beta_2 = \frac{L - 0.77\sqrt{\Delta l(4a - \Delta l)}}{L}$$

$$x_2 = \frac{(A^{11}C^{11})^2 + (B^{11}C^{11})^2 - (AB)^2 - (BB^{11})^2}{2(A^{11}C^{11})(B^{11}C^{11})} + \frac{2(AB)(BB^{11})\cos \beta_1}{2(A^{11}C^{11})(B^{11}C^{11})}$$

$$A^{11}C^{11} = 0.75W_f$$

$$B^{11}C^{11} = \frac{0.86W_f \sqrt{0.87L\sqrt{F_5} - 0.34F_5}}{1.5L - 1.16\sqrt{F_5}}$$

$$F_5 = \Delta l(4a - \Delta l)$$

$$AB = 0.866W_f ; BB^{11} = \frac{0.65W_f L}{1.5L - 1.16\sqrt{F_5}}$$

$$\cos \beta_1 = \frac{0.5L + 0.77\sqrt{F_5}}{L}$$

Substituting the formulae of (5) and (6) into the formula of (4) and further deriving it, will end up to an expression of plastic load carrying capacity  $(F_{ax})_{pl}$  as written below:

$$(F_{ax})_{pl} = \frac{-c_2 + \sqrt{c_2^2 + 4c_1c_3}}{2c_1} \quad (10)$$

The above equation is the expression of plastic load carrying capacity in term of axial shortening  $(\Delta l)$  and the values of  $c_1$  to  $c_3$  can be seen in the following formulations.

$$*c_1 = \frac{c_{11}c_{12}}{c_{13}(c_{14} - c_{15})} + \frac{c_{16}}{c_{17}} ; *c_2 = \Delta l$$

$$*c_3 = c_{11}xc_{31}(c_{14} - c_{15}) + \frac{c_{32}(\theta_1 + \theta_2)}{c_{17}}$$

$$c_{11} = 2 \tan^{-1} \left( \frac{2a - \Delta l}{\sqrt{\Delta l(4a - \Delta l)}} \right) ; c_{12} = a(W_f - 2y_c)^2$$

$$c_{13} = 0.72\sigma_y W_f^2 W_w^2 ; c_{14} = \ln \tan \left( \frac{\pi}{4} + \frac{\phi_1}{2} \right)$$

$$c_{15} = \ln \tan \left( \frac{\pi}{4} + \frac{\phi_2}{2} \right) ; c_{16} = y_c^2 (\theta_1 + \theta_2)$$

$$c_{17} = 1.73\sigma_y W_f^3 ; c_{31} = \frac{0.045\sigma_y t^2 W_w^2}{a}$$

$$c_{32} = (0.866\sigma_y + W_f^2)^2$$

Iterating the value of axial shortening  $(\Delta l)$  in the above equation will generate the behaviour of unloading load-deflection relationship, which is called a plastic mechanism curve. In case of the value of  $\Delta l$  is equal to 0 (zero), the formula of (10) becomes:

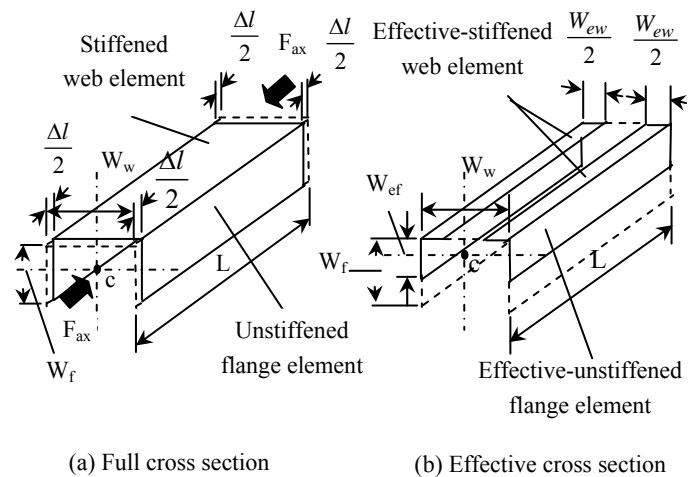
$$(F_{ax})_{pl} \text{ at } (\Delta l = 0) = \left\{ \ln \tan \left( \frac{\pi}{4} + \frac{\phi_1}{2} \right) - \ln \tan \left( \frac{\pi}{4} + \frac{\phi_2}{2} \right) \right\} \times \frac{0.18\sigma_y t W_f W_w^2 \sqrt{a}}{a(W_f - 2y_c)} \quad (11)$$

Table 2 and Figure 14 show that the value of  $(F_{ax})_{pl}$  at  $(\Delta l = 0)$  calculated using the above equation is quite close to a squash load  $(F_s)$  calculated using:

$$F_s = \sigma_y t (W_w + 2W_f) \quad (12)$$

## 2.2 Elastic Analysis

The previous section has discussed that in the elastic analysis of the beam, the effect of local buckling is necessarily considered by adopting an effective width concept. This concept is applied to analyse a compressed element, which is still effective in carrying applied loads. In the investigated beam subjected to axial compressions, both its elements of web and flanges are of compressed ones. These elements have to be determined their effective width dimensions because in the elastic analysis, the section properties of the beam will be determined according to its effective cross section instead of its full cross section. An effective cross section of the beam  $(A_{ef})$  as shown in Figure 4 is the fundamentals of elastically developing a formula of the load carrying capacity of the beam in term of its axial shortening. Procedures of determining the effective width of web  $(W_{ew})$  and flange  $(W_{ef})$  in the Figure 4 refer to the rules as specified in the reference of British Standard (BS 5950 1987).



**Figure 4. Full and effective cross sections of the investigated beam.**

The web is a stiffened element and its effective width ( $W_{ew}$ ) is determined as follows:

$$\text{If } \frac{f_c}{p_{cr}} < 0.123 ; W_{ew} = W_w \quad (13)$$

$$\text{If } \frac{f_c}{p_{cr}} \geq 0.123 ; W_{ew} = W_w \left[ 1 + 14 \left\{ \sqrt{\frac{f_c}{p_{cr}}} - 0.35 \right\}^4 \right]^{-0.2}$$

$f_c$  is a compressive stress in the effective element and it can be equated to design strength ( $p_y$ ) or yield strength ( $\sigma_y$ ). Meanwhile,  $p_{cr}$  is a local buckling stress and calculated from:

$$p_{cr} = 185000 K \left( \frac{t}{W_w} \right)^2 \quad (14)$$

$K$  is a buckling constant and the constant for the stiffened element of web ( $K_{st}$ ) is computed using:

$$K_{st} = \frac{2}{\beta} + \frac{2 + 4.8h}{\beta^2} ; h = \frac{W_f}{W_w} ; \beta = (1 + 15h^3)^{0.5} \quad (15)$$

The effective width of flange element ( $W_{ef}$ ) is also calculated according to the same procedure as described in equation (13) and (14) except the values of  $W_{ew}$  and  $W_w$  in both formulae are substituted by those of  $W_{eff}$  and  $W_f$ . A buckling constant of the unstiffened flange element ( $K_{unst}$ ) is determined from the following equation and  $W_{eff}$  obtained is then used to calculate the  $W_{ef}$ .

$$K_{unst} = K_{st} h^2 ; W_{ef} = 0.89W_{eff} + 0.11W_f \quad (16)$$

Ramberg and Osgood have developed a formula (17) to plot a non-linear material stress-strain curve (Lau & Hancock 1989). The elastic analysis basically uses the formula (17) to estimate elastic load-deflection behaviour of the investigated beam in this paper.

$$\varepsilon = \frac{\sigma}{E} + \frac{3\sigma}{7E} \left( \frac{\sigma}{\sigma_{0.7}} \right)^{(n-1)} ; n = 1 + \frac{\log\left(\frac{17}{7}\right)}{\log\left(\frac{\sigma_{0.7}}{\sigma_{0.85}}\right)} \quad (17)$$

$\sigma_{0.7}$  and  $\sigma_{0.85}$  are stresses corresponding to  $E_s = 0.7 E$  and  $E_s = 0.85 E$  where  $E$  is an elastic modulus of the basic material. These stresses are determined using stress-strain behaviour of the basic material obtained from tensile tests. The elastic analysis of the investigated beam using the above equation was carried out in two stages, which consist of linear-elastic analysis and non-linear elastic (Inelastic) one. Both stages are aimed at developing a formula of elastic load carrying capacity ( $(F_{ax})_e$  in term of axial shortening ( $\Delta l$ ) relationship. In the first stage, the first term in the right hand side of equation (17), which relates to Hooke's law, is further analysed to get the following linear-elastic load-deflection relationship.

$$(F_{ax})_{e(linear)} = \frac{Et(W_{ew} + 2W_{ef})\Delta l}{L} \quad (18)$$

In the meantime, the non-linear elastic load-deflection one is obtained from analysing the second term of the right hand side of equation (17) to get its formulation as follows:

$$(F_{ax})_{e(non-linear)} = (\Delta F_{ax})_{inel} + F_{0.7} \quad (19)$$

$$F_{0.7} = \sigma_{0.7} t (W_{ew} + 2W_{ef})$$

$$F_6 = 7 E \sigma_{0.7}^{(n-1)} \{t(W_{ew} + 2W_{ef})\}^n$$

$$(\Delta F_{ax})_{inel} = \left[ \frac{F_6 (\Delta l - \Delta l_{0.7})}{3L} \right]^{\frac{1}{n}} \quad (20)$$

$\Delta l_{0.7}$  is axial shortening that corresponds to  $F_{0.7}$  and equations (10), (18), (19) and (20) are iterated using the written computer program to implement the method of cut-off strength in estimating the axial-compressive strength of the investigated beam.

### 3. EXPERIMENTAL INVESTIGATION

In the experimental investigation, tensile tests were initially performed to assess mechanical properties of the basic material used to manufacture the thin-walled channel steel section beam. The basic material is of a carbon steel sheet of Standard JIS G 3141 – SPCC and tensile test specimens are designed according to Standard JIS Z 2201 No. 13A (See Figure 5). The tensile tests were conducted on a testing machine RME 100 Schenck Trebel whose maximum capacity is 100 kN. The tensile specimens were tested in a room temperature to fracture and during the tests, a relationship of static-tensile load to specimen deformation was always monitored by means of extensometer that was mounted at a gauge length of 100 mm.

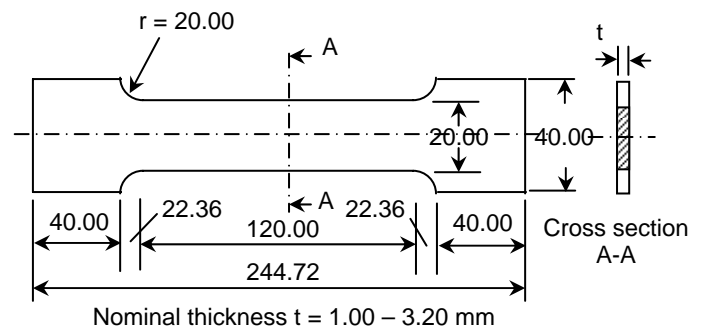
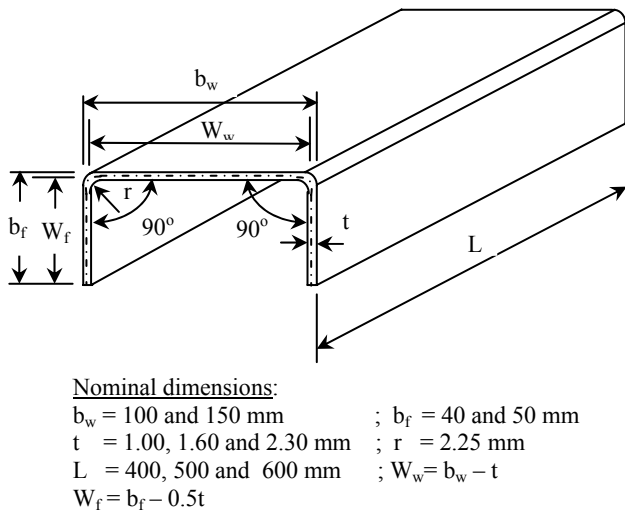


Figure 5. Design of tensile test specimen (JIS 1995).



**Figure 6. Design of axially compressed-tested specimen** (Setiyono 2001)

The mechanical properties of the basic material can be identified by evaluating the tensile test load-deformation behaviour obtained and their values, on average, are as follows (Setiyono 2001) :

- Ultimate tensile strength ( $\sigma_{UTS}$ ) = 322.25 MPa
- Yield strength ( $\sigma_y$ ) = 191.50 MPa
- Modulus of elasticity ( $E$ ) =  $196.45 \times 10^3$  MPa
- Stress corresponding to  $E_s = 0.7 E$  , ( $\sigma_{0.7}$ ) = 134.33 MPa
- Stress corresponding to  $E_s = 0.85 E$  , ( $\sigma_{0.85}$ ) = 115.67 MPa

A subsequent step of the experimental investigation is axial-compressive tests on 38 specimens of thin-walled channel steel section beam. The specimen is cold-formed from the carbon steel sheet JIS G 3141 – SPCC as above mentioned and its detail design can be seen in the above Figure 6. The axial-compressive tests were also performed in an ambient temperature using the testing machine RME 100 Schenck Trebel of a 100 kN maximum capacity until the beam specimens completely failed. In order to ascertain that the beam specimens are really subjected to axial-compressive test loads, they are located in-between the upper and lower clamping devices in such away that the center line of the devices exactly coincides to the longitudinal center line of the specimens. This test arrangement is shown in Figure 7 and it is clearly seen that the LVDTs are used to measure axial shortening as well as lateral deflection of the web element. Actual behaviour of load-deflection relationship was always monitored during the tests and plotted in X-Y recorders. The axial-compressive strength of the tested specimens was measured from a load-indicating device of the testing machine and also from a maximum test load of the experimental load-deflection behaviour obtained. A mode of failure at each specimen is carefully observed and this repeatedly occurs in the form of local plastic failure mechanisms as indicated in Figure 8.

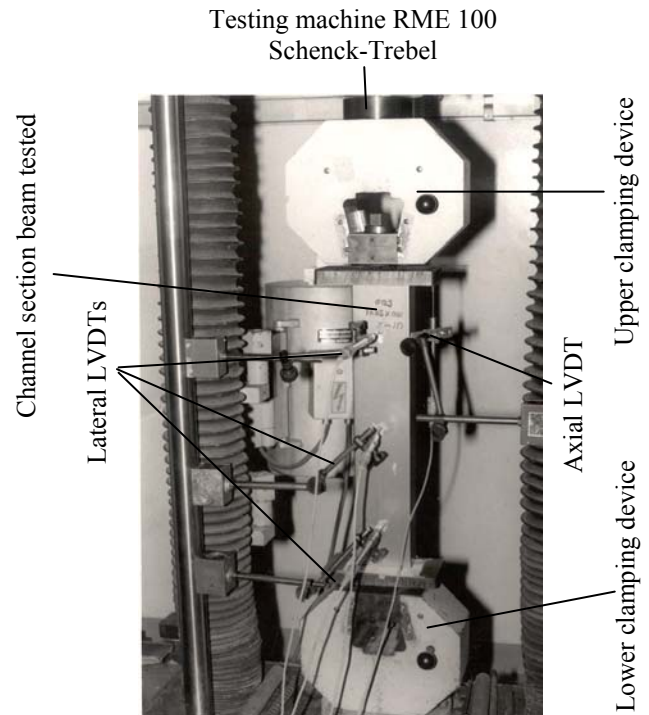


**Figure 7. Configuration of axial-compressive tests** (Setiyono 2001)

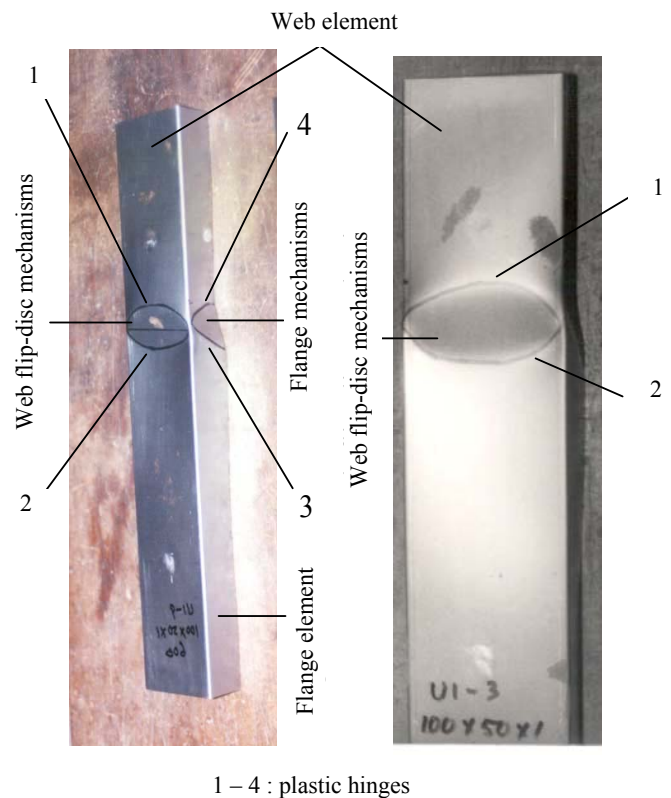


**Figure 8. Local-plastic failure mechanisms of the tested beam** (Setiyono 2001)

#### 4. VERIFICATION OF ANALYTICAL RESULTS

The axial-compressive strength of the beam estimated using the analytical approach developed in

this research program is verified by comparing it to actual data measured in the tests. Table 1 indicates the comparison of individual data of estimated and actual strength of 38 thin-walled channel steel section beams axially-compressively loaded. The ratio of the individual-experimental-axial-compressive strength ( $F_{ex}$ ) and theoretical one ( $F_{th}$ ) is also plotted in terms of web ratio ( $W_w/t$ ) and flange ratio ( $W_f/t$ ) as shown in Figure 9 and 10. It is clearly seen in the Figures that this ratio data, which also expresses the percentage of deviation between estimated and actual strength, still lies within an acceptable limits of  $\pm 20\%$  and mostly scatters in the conservative region ( $1.00 \leq [F_{ex}/F_{th}] \leq 1.20$ ). According to a statistical analysis of the scattered deviation data, its mean value is 1.03 with the standard deviation of 0.058. These statistical measures mean that the average estimated strength tends to underestimate the actual one by 3% and this is of course a considerably safe prediction. Figures 11-13 show theoretical load-deflection behaviour of the investigated beam and this is represented by the plastic mechanism and elastic curves. The plastic mechanism curve is established by iterating equation (10), whereas the equations (18), (19) and (20) are iterated to establish the elastic one.

**Table 1. Comparison of theoretical and actual strength**

Specimen Designation	$\frac{b_f}{t}$	$\frac{b_w}{t}$	L in mm	Axial-compressive strength (kN)		$\frac{F_{ex}}{F_{th}}$
				$F_{th}$	$F_{ex}$	
U1-1(100x40x1)	40.82	101.82	400	16.06	16.00	≈1.00
U1-6(100x40x1)	42.93	106.11	500	14.62	15.00	1.03
U1-7(100x40x1)	40.87	101.96	600	15.63	16.40	1.05
U1-3(100x50x1)	51.16	101.98	400	15.43	17.15	1.11
U1-4(100x50x1)	50.20	99.90	500	15.81	17.20	1.09
U1-9(100x50x1)	48.82	98.12	599	16.17	17.80	1.10
U1-3(150x50x1)	51.57	154.64	400	18.02	17.20	0.95
U1-4(150x50x1)	50.06	149.70	500	18.79	18.40	0.98
U1-7(150x50x1)	51.04	152.86	600	17.86	18.70	1.05
U1-3(100x40x1)	40.06	99.94	400	16.61	16.80	1.01
U1-5(100x40x1)	40.76	101.22	500	15.83	16.30	1.03
U1-4(100x40x1)	41.56	104.06	600	15.10	17.20	1.14
U1-5(100x50x1)	50.00	99.90	500	15.79	15.50	0.98
U1-7(100x50x1)	50.01	99.68	600	15.62	17.30	1.11
U1-1(150x50x1)	50.14	150.15	400	19.00	18.30	0.96
U1-1(100x50x1)	53.00	106.21	400	14.35	16.50	1.15
U1-8(150x50x1)	49.80	150.00	600	18.49	17.00	0.92
U1.6-5(100x40x1.6)	24.88	62.50	500	38.33	37.50	0.98
U1.6-7(100x40x1.6)	25.33	63.27	600	37.53	37.20	≈1.00
U1.6-4(100x40x1.6)	25.13	62.50	500	38.21	37.50	0.98
U1.6-2(100x40x1.6)	25.35	63.38	400	38.10	38.50	1.01
U1.6-7(100x50x1.6)	31.65	63.35	600	35.29	36.00	1.02
U1.6-4(100x50x1.6)	31.13	62.73	500	36.68	37.00	1.01
U1.6-1(100x50x1.6)	32.53	64.96	400	34.53	38.00	1.10
U1.6-8(150x50x1.6)	32.93	98.62	600	39.11	37.50	0.96
U1.6-4(150x50x1.6)	33.36	100.00	500	38.87	39.25	1.01
U2.3-6(100x40x2.3)	17.52	43.82	500	63.71	71.00	1.11
U2.3-5(100x40x2.3)	17.53	43.30	500	64.44	66.75	1.04
U2.3-4(150x50x2.3)	22.66	68.14	500	77.26	83.50	1.08
U2.3-3(150x50x2.3)	22.65	68.14	500	77.25	83.00	1.07
U2.3-2(100x50x2.3)	21.57	43.43	400	67.26	71.75	1.07
U2.3-3(100x40x2.3)	17.30	43.50	400	66.39	71.25	1.07
U2.3-2(150x50x2.3)	21.70	64.96	400	84.51	84.50	1.00
U2.3-3(150x50x2.3)	21.24	64.04	400	84.64	80.00	0.95
U2.3-1(150x50x2.3)	22.03	65.90	401	82.55	83.75	1.01
U2.3-8(100x40x2.3)	17.46	43.80	400	65.70	72.50	1.10
U2.3-8(150x50x2.3)	21.90	65.79	600	81.19	84.30	1.04
U2.3-9(150x50x2.3)	21.88	65.75	600	81.50	80.00	0.98

$F_{th}$  : theoretically axial-compressive strength  
 $F_{ex}$  : experimentally axial-compressive strength

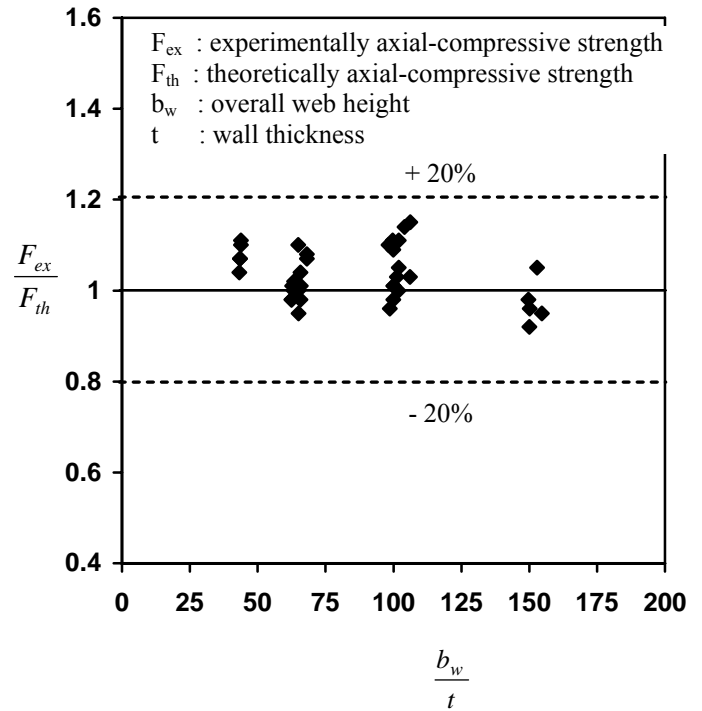


**Figure 9. Scattered deviation of theoretical and actual strength comparison in term of the web ratio.**

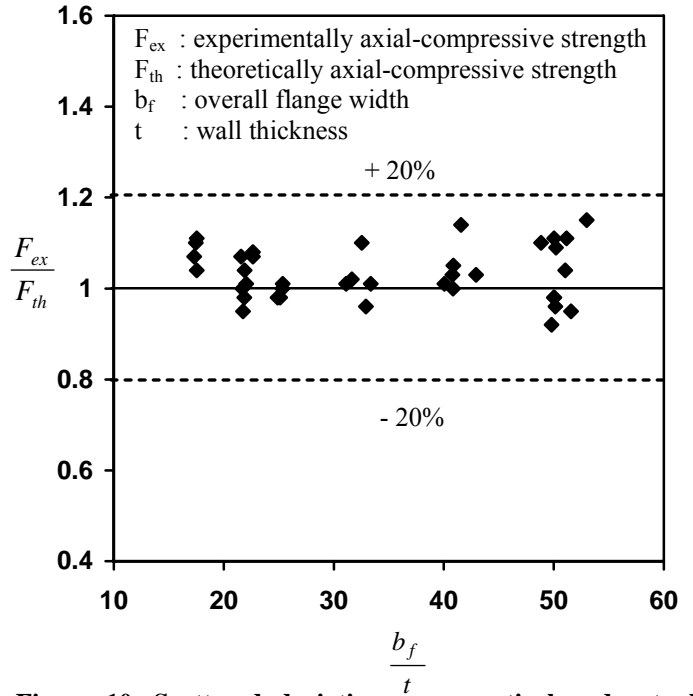


**Figure 10. Scattered deviation of theoretical and actual strength comparison in term of the flange ratio.**

On the comparison of the theoretical load-deflection curve to the experimental one, it can be seen that the actual elastic behaviour is well predicted by the one obtained from the elastic-analytical approach. Meanwhile, the post-collapse behaviour of the beam can be predicted by the plastic mechanism

(Unloading) curve with fairly accurate and the prediction tends to underestimate it. The reasons of this underestimated prediction can be explained as follows:

- The test results show that the local-plastic failure mechanism of the beam is not always formed exactly at its mid-span as assumed in the analytical approach
- The effect of strain hardening is not taken into account in the analysis at the plastic hinge zones and the material is assumed to follow the elastic-perfectly-plastic stress-strain behaviour.

As stated in the method of cut-off strength, Figures 11-13 also indicate that the analytical axial-compressive strength to be determined as the elastic behaviour curve has been intercepted by the plastic mechanism one. The maximum plastic load carrying capacity indicated by the value at the intersection between the plastic mechanism curve and the vertical axis is equal to a squash load. A calculation of this load using either equation (11) or (12) produces similar values as can clearly be seen in Table 2 and plotted in Figure 14. In this Figure, the different data calculated using both equations are scattered quite closely to the solid diagonal line. Table 2 also indicates that the ratio of data obtained from equations (11) and (12) is nearly unity because the data differs only by 2% and this can be considered as insignificant differences. Thus, it can be certainly found out that both equations (11) and (12) can actually be used to determine the value of squash load.

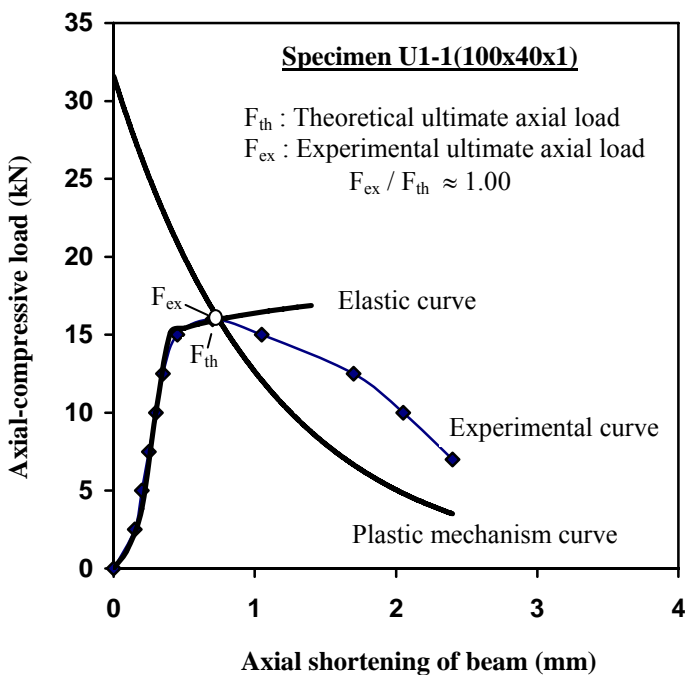


Figure 11. Theoretical and actual load-deflection behaviour (Nominal  $t = 1.00$  mm).

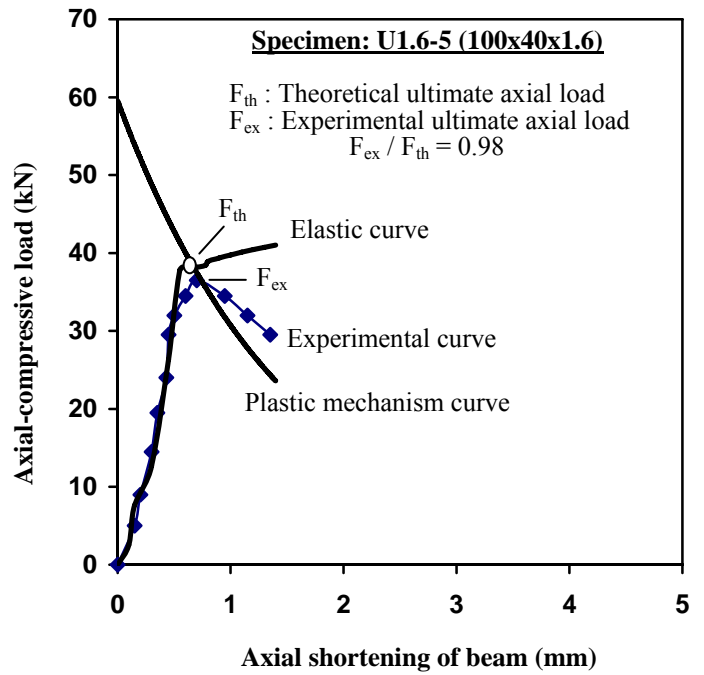


Figure 12. Theoretical and actual load-deflection behaviour (Nominal  $t = 1.60$  mm).

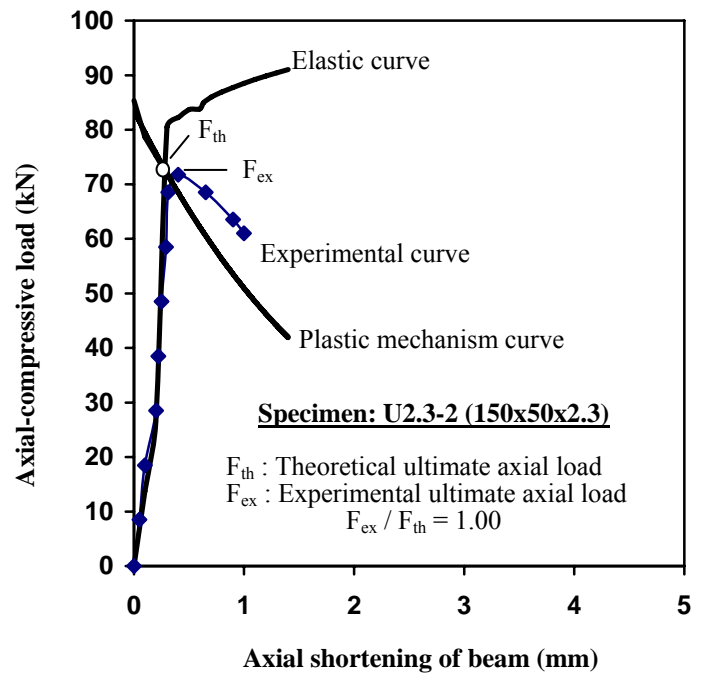


Figure 13. Theoretical and actual load-deflection behaviour (Nominal  $t = 2.30$  mm).

**Table 2. Comparison of equation (11) and (12)**

Specimen Designation	$\frac{b_f}{t}$	$\frac{b_w}{t}$	L in mm	Plastically axial load carrying capacity at $\Delta l = 0$ (kN)		$\frac{(F_{ax})_{pl}}{F_s}$
				$(F_{ax})_{pl}$	$F_s$	
				U1-1(100x40x1)	40.82	101.82
U1-6(100x40x1)	42.93	106.11	500	32.80	32.14	1.02
U1-7(100x40x1)	40.87	101.96	600	34.10	33.42	1.02
U1-3(100x50x1)	51.16	101.98	400	37.95	37.21	1.02
U1-4(100x50x1)	50.20	99.90	500	38.73	37.97	1.02
U1-9(100x50x1)	48.82	98.12	599	39.37	38.61	1.02
U1-3(150x50x1)	51.57	154.64	400	47.00	46.09	1.02
U1-4(150x50x1)	50.06	149.70	500	48.40	47.46	1.02
U1-7(150x50x1)	51.04	152.86	600	47.44	46.52	1.02
U1-3(100x40x1)	40.06	99.94	400	34.80	34.10	1.02
U1-5(100x40x1)	40.76	101.22	500	33.92	33.24	1.02
U1-4(100x40x1)	41.56	104.06	600	33.35	32.68	1.02
U1-5(100x50x1)	50.00	99.90	500	38.65	37.90	1.02
U1-7(100x50x1)	50.01	99.68	600	38.61	37.86	1.02
U1-1(150x50x1)	50.14	150.15	400	48.52	47.57	1.02
U1-1(100x50x1)	53.00	106.21	400	38.65	37.90	1.02
U1-8(150x50x1)	49.80	150.00	600	48.36	47.42	1.02
U1.6-5(100x40x1.6)	24.88	62.50	500	55.16	54.05	1.02
U1.6-7(100x40x1.6)	25.33	63.27	600	54.61	53.51	1.02
U1.6-4(100x40x1.6)	25.13	62.50	500	55.41	54.29	1.02
U1.6-2(100x40x1.6)	25.35	63.38	400	54.69	53.59	1.02
U1.6-7(100x50x1.6)	31.65	63.35	600	60.77	59.59	1.02
U1.6-4(100x50x1.6)	31.13	62.73	500	61.49	60.29	1.02
U1.6-1(100x50x1.6)	32.53	64.96	400	59.30	58.14	1.02
U1.6-8(150x50x1.6)	32.93	98.62	600	73.32	71.89	1.02
U1.6-4(150x50x1.6)	33.36	100.00	500	72.39	70.97	1.02
U2.3-6(100x40x2.3)	17.52	43.82	500	78.09	76.53	1.02
U2.3-5(100x40x2.3)	17.53	43.30	500	78.95	77.36	1.02
U2.3-4(150x50x2.3)	22.66	68.14	500	105.36	103.30	1.02
U2.3-5(150x50x2.3)	22.65	68.14	500	105.34	103.28	1.02
U2.3-2(100x50x2.3)	21.57	43.43	400	87.38	85.68	1.02
U2.3-3(100x40x2.3)	17.30	43.50	400	78.69	77.10	1.02
U2.3-2(150x50x2.3)	21.70	64.96	400	109.88	107.73	1.02
U2.3-3(150x50x2.3)	21.24	64.04	400	108.04	107.91	1.02
U2.3-1(150x50x2.3)	22.03	65.90	401	108.65	106.53	1.02
U2.3-8(100x40x2.3)	17.46	43.80	400	77.94	76.37	1.02
U2.3-8(150x50x2.3)	21.90	65.79	600	109.25	107.11	1.02
U2.3-9(150x50x2.3)	21.88	65.75	600	109.15	107.02	1.02

$(F_{ax})_{pl}$  : plastically axial load carrying capacity at  $\Delta l = 0$  calculated using equation (11)

$F_s$  : squash load calculated using equation (12)

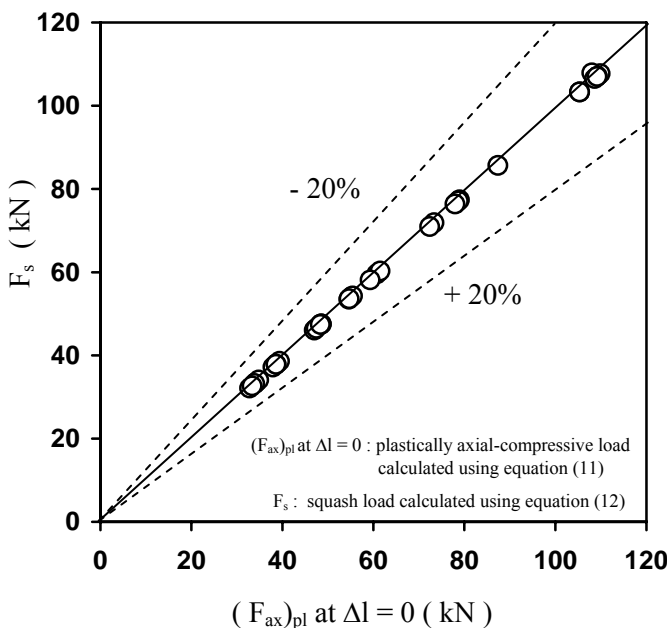


**Figure 14. Comparison of equation (11) and (12).**

## 5. CONCLUSIONS

A combined method of plastic mechanism and elastic approaches has been developed to analyse the strength of a thin-walled channel steel section beam subjected to axial compressive loads. The plastic mechanism approach is performed on the basis of an energy equilibrium concept applied to the analysis of an idealized plastic failure mechanism model of the beam. In the elastic approach, the effect of local buckling on the compressed elements is taken into account by adopting an effective width concept in determining the cross section of the beam, which is still effective to carry applied-compressive loads. The strength of the investigated beam is estimated by implementing the method of cut-off strength on the two different curves of plastic and elastic load carrying capacity. The accuracy of using the method developed is also assessed by comparing its predicted results to actual ones measured in axial compression tests of thin-walled channel steel section beam specimens. The assessment has indicated that the analytical model presented in this paper can predict the axial-compressive strength quite well and tends to underestimate the actual strength by 3%. The analytical model also shows to be able to estimate load-deflection behaviour of the beam, which is very close to the actual behaviour displayed from the test results.

## ACKNOWLEDGEMENTS

The research program reported herein is financed by the Indonesian Government through the project framework in the Agency for the Assessment and Application of Technology (BPPT). Valuable contributions rendered by engineers and technicians in the Technology Center for Structural Strength (B2TKS-BPPT) especially in the experimental investigation are gratefully acknowledged. The author also thanks P.T. Duta Laserindo Metal – Sheet Metal Job in Bekasi – Indonesia for manufacturing a number of specimens used to support the research activities.

## REFERENCES

Bakker, M.C.M. "Yield line analysis of post-collapse behaviour of thin-walled steel members", Heron, Vol.35, No.3, 1990, pp. 3-50.

- British Standard Institution, "Structural use of steelwork in building, Part 5. Code of practice for design of cold-formed sections", BS 5950, 1987.
- Japanese Standards Association, "JIS Handbook – ferrous materials & metallurgy I", 1995, pp. 34.
- Japanese Standards Association, "JIS Handbook – ferrous materials & metallurgy II", 1995, pp. 253-272.
- Lau, S.C.W. and Hancock, G.J., "Inelastic buckling analyses of beams, columns and plates using the spline finite strip method", *Thin-Walled Structures* 7, 1989, pp. 213-238.
- Mahendran, M., "Local plastic mechanisms in thin steel plates under in-plane compression", *Thin-Walled Structures*, Vol.27, No.3, 1997, pp. 245-261.
- Murray, N.W. and Khoo, P.S., "Some basic plastic mechanisms in the local buckling of thin-walled steel structures", *International Journal of Mechanical Sciences*, Vol.23, No.12, 1981, pp. 703-713.
- Murray, N.W., "Introduction to the theory of thin-walled structures", *Oxford Engineering Sciences Series* 13, 1986, pp. 313.
- Rhodes, J., "Design of cold-formed steel members", Elsevier Science Publishers Ltd., 1991.
- Setiyono Harkali, "Web crippling of cold-formed plain channel steel section beams", PhD Thesis, University of Strathclyde, August, 1994, pp. 199-234.
- Setiyono Harkali, "Application of plastic mechanism approach to analyse the strength of a light gauge steel section", *Proceedings – The Tenth International Pacific Conference On Automotive Engineering (IPC-10)*, Melbourne-Australia, May 23-28, 1999, pp. 53-58.
- Setiyono Harkali, "The Development of an analytical model for the strength of light gauge steel structures", Final Research Report, Agency for the Assessment and Application of Technology (BPPT), 2001. (Translated from Indonesian language)
- Setiyono Harkali, Karmiadji Djoko W. and Anton, A., "The Development of a combined plastic mechanism and elastic-analytical model to estimate the moment capacity of a thin-walled channel section (IPC2001D081)", *Proceedings (CD-ROM) – The Eleventh International Pacific Conference On Automotive Engineering (IPC-11)*, Shanghai-China, Nov. 8-9<sup>th</sup>, 2001.
- Setiyono Harkali and Rachman Abdul, "A plastic mechanism approach in an analytical model to estimate the strength of a lightweight steel structure", *Proceedings – 21<sup>st</sup> Conference of Asean Federation of Engineering Organizations (CAFEO – 21)*, Yogyakarta, 22-23 October, 2003, pp. 1/15-15/15.